Concrete Beton

Number 124
March 2010

The Official Journal of
The Concrete Society
of Southern Africa

CONCRETE SOCIETY
OF SOUTHERN AFRICA

Platinum members: AfriSam
Lafarge

Accredited technical paper:
Flexural Design of Fibre Reinforced Concrete

Fulton Award Winner:
Berg Water Project

Concrete News and events

AfriSam

LAFARGE

President's Message

It is with a touch of melancholy that I write this, my last President's message for the Concrete Beton as my term of office is coming to an end during this month. When reflecting back upon the last two years' events there have been many highlights.

Foremost amongst these for me however, is the new administrative office that was realised. Natasja Pols joined us in about July 2008 and Jeanine Steenkamp (nee Kilian) in November of that year. With these two highly effective and vibrant individuals, the Society's administration has stepped up several notches.

The last two-year period also marks the introduction of the new 'Company Membership' option. This move was embarked upon, after a large amount of brainstorming and deliberation by the Council in order to transform the Society into a much more financially sustainable entity.

This initiative has proved highly successful and currently we have 2 platinum, 3 gold, 4 silver and 13 bronze members signed up.

I would again just like to express our gratitude towards our company members and bid them welcome.

Since taking over at the helm of the Society, I have had the pleasure of observing two superlative national events: the first being the Self Compacting Concrete (SCC) Seminar Road-show which was hosted at all four of the branches, the second was at the end of last year with the University of Stellenbosch.

The Society hosted the Advanced Concrete Materials conference, which attracted speakers from across the world.

In attending both events, I can decisively state that both these events were World Class. Obviously the zenith of my two-year stint as President of the Society is the Annual Fulton Awards. The event, held over the weekend of 19-21 June 2009 was fabulous. However for me, the actual site visits and mixing with the professional teams involved in the projects and being infected by their absolute passion and dedication to their respective projects is what will remain emblazoned on my memory for ever.

This dedication is what makes me eternally grateful to be part of the Southern African Construction Industry in general and the Concrete and Cement Industry in particular.

Francois Bain Pr Eng
President:
The Concrete Society of Southern Africa

Cover: Aurecon Group
Peter Mokaba Stadium
Page 16.

Issue 123: The Self Compacting Cement headline should have read Self Compacting Concrete.

FULTON AWARDS WINNER

Berg Water Project

The magnificent Berg Water Project near Franschoek for the Trans-Caledon Tunnel Authority earned kudos for the principal agent, Berg River Consultants, contractor Berg River Projects Joint Venture and subcontractor the Department of Water Affairs and Forestry. The impressive Berg Water Project in the Western Cape proved a worthy winner of the Fulton Awards Civil Engineering Project category.

Lengthy research on issues of sustainability, water storage, supply infrastructure and durability contributed to the winning design and construction of the Berg River dam project.

Achieving the critical impoundment date for the Berg River dam in July 2007 was testimony to the wise decision taken in 2003 to construct the embankment as a concrete-faced rockfill dam (CFRD) and foreshadowed the first filling and commissioning of the dam by August 2008. The growing population and demand for water in the Western Cape and in the greater Cape Town metropolis required constructing the multi-faceted, R1,6bn Berg Water Project which will add 81 million m³ of water annually, representing an 18% increase to the existing water system. The project is the largest conventional water resource in the region.

The early dam-type selection process had identified the CFRD as the preferred option, based on clear construction and programming advantages that would be experienced in the three wet winters of the 36 month critical path duration.

The project required 64000 m² of reinforced concrete face-slabs, 100 km of extruded concrete kerbs and a further 20 000 m³ of reinforced concrete for the perimetric plinth, wave-wall and end structures to the embankment.

The design for this unique structure, a first for South Africa, was to build a stable concrete plinth on the weathered and jointed bedrock, through comprehensive cementitious sub-surface grouting which also assured water-tightness.

Civil Engineering Fulton Winner

Connection of the face slab to this comparatively rigid plinth required a uniquely engineered joint that allowed deflections and distortions to 100 mm, given the settlement of the embankment with respect to time.

Conventional design approaches to other structures followed precedent in the extensive use of concrete as the most appropriate construction material for the 63 m high intake tower, uniquely providing both wet and dry-well vertical chambers. The 158 m long, 5,5m diameter bottom outlet conduit releases 200 m^3/s. The spillway ogee crest, splitters, galleries and deep fast-flowing (25 m/s) discharge chute culminates in an energy-dissipating flip-bucket deflector above the plunge pool. The Berg Water Project is the primary framework for two large pump stations 10km downstream at Dasbos and Drakenstein. There are six large gauging weirs, an irrigation release structure and the complex sedimentation and water abstraction works at Drakenstein. The design included the cement-mortar lining of 12,2 km of steel pipe (1,5 m diameter) and many ancillary reinforced concrete chambers, thrust blocks, etc. The entire project used some 150 000 m^3 of concrete.

Special features and challenges included the use of local aggregate sources; the need for long term concrete durability in the corrosive soft mountain waters; optimisation of pipe linings, wet-well/conduit requirements, spillway performance and shape and downstream abstraction works, using extensive physical model studies; optimisation of structures like the intake tower, outlet conduit and embankment, using finite element analyses and long term monitoring using permanent instrumentation arrays and read-out facilities.

The focus on excellence in all aspects of management, design, construction and control, applied in every aspect of concrete production, handling, casting and finishing, has produced an outstanding product.

FULTON AWARDS WINNER

Judges' Citation

The degree of attention given to both design and construction aspects was truly outstanding. The consideration given at concept stage to issues of sustainability, co-ordination with other water storage and supply infrastructure and durability is exemplary.

The choice of a concrete faced, rock-fill dam in order to meet time constraints proved highly successful.

The judges were also impressed by the extensive length over which the design studies were taken, including earthquake studies on the dam wall and the phenomenal intake tower structure, as well as the comprehensive hydraulic modelling performed on both the dam infrastructure and the Drakenstein abstraction works. The team must be commended on the high quality finish required and achieved in forming the ogee arch to the spillway in particular. Lastly, special note must be taken of the training of local community members and who, with the new skills obtained, will surely be of benefit to the Franschoek community. The multi-facetted Berg Water Project is a worthy recipient of the Fulton Award for the Civil Engineering category in 2009.

PPC's JSE parnership

PPC, the giant cement producer, celebrated its 100 year anniversary on the Johannesburg Stock Exchange during February.

The iconic company traced its history back to President Paul Kruger inaugurating the turning of the soil at the Pretoria plant in 1890, to its current history and production of 8 million tons of cement and aggregates a year from its eight plants.

Chairman, Bheki Sibiya and his team tracked the company's growth and highlighted the importance of its product in construction of the seat of power in Pretoria, the Union Buildings, and supplying 250 000 bags of cement in the building of Hartebeespoort Dam.

CEO, Paul Stuiver says that PPC has four ingredients in its recipe for success. First – the longevity of the product has proved it is a key building material that has shaped the world. Demand for the product is insatiable. Secondly - the vision and courageous leadership in the past kept their eye on the long term goals of business and mining operations with a strategic 30,40,50 year time frame. The company has survived two World Wars, a depression and oil crises.

Thirdly – the passion of the people who work at PPC – "It's like a family business and the company was recognised in a Deloittes' survey as the Best Company to work for. This accolade was well deserved as two of the current executives and family members gave 70 and 75 years of service."

"This has kept us ahead of the opposition for 100 years."And lastly - the final ingredient is the long term relationships between shareholders, advisors and customers. The German company which supplied building equipment in 1906 still retains and supplies PPC, the 1910 share register reflects a board meeting minuted by Bowman Gilfillan, PPCs trusted legal advisor, the mining companies from the 1880s and 1890s continue to use PPC today. In 1906 the company's income exceeded its expenditure. The giant cement manufacturer supplied Spoornet with material for harbour projects. PPC has come a long way from when 1960 shares were traded between 4,75cents to 8,3cents, while today they are standing at R32,80.

Joe Shibambo, Bheki Sibiya, Paul Stuiver, Salim Abdul Kader and Sello Helepi

Chairman, Sibiya opened trading for the day by blowing the Kudu horn, when handed the horn the JSE spokesperson joked that the strength and power of the echo correlates to how well the company performs.

Sibiya proved he was certainly up to the task and it bodes well for a highly lucrative future, longevity and success for the company into the future.

Kgathola Ngoasheng

Flexural Design of Fibre Reinforced Concrete

by Chote Soranakom and Barzin Mobasher

Chote Soranakom is a post-doctoral fellow in the Department of Civil and Environmental Engineering at Arizona State University. His interests are in the area of fibre and fabric reinforced concrete materials and mechanical modelling of composite systems. **Barzin Mobasher** is a professor in the Department of Civil and Environmental Engineering at Arizona State University. He has more than 20 years of research experience in engineering materials. Mobasher is a member of American Concrete Institute committees 446, 544, and 549.

ABSTRACT: A set of closed form design equations for flexural design of fibre reinforced concrete are presented. These equations are based on simplified tensile and compressive constitutive response and may be used in a limit state approach or serviceability-based criterion that limits the effective tensile strain capacity. The equations allow generation of flexural moment-curvature response of a rectangular beam section for use in structural analysis calculations in addition to design charts for strain softening fibre reinforced concrete. To prevent sudden failure after flexural cracking and to control crack width, equations for minimum post-crack tensile strength are also proposed. The analytical tensile strain equations proposed for serviceability limit the average crack width of structural members. In addition, the bi-linear moment-curvature model is used in conjunction with geometrical relationship between curvature and deflection to determine short-term deflections of structural members. An example of a one-way slab demonstrates the calculation steps.

Keywords:

composite concrete flexural members; design; fibre reinforced concrete

INTRODUCTION

Fibre reinforced concrete (FRC) can be considered as a brittle matrix composite material consisting of cementitious matrix and discrete fibres. The fibres that are randomly distributed in the matrix act as crack arrestors. Once the matrix cracks under tension the debonding and pulling out of fibres dissipate energy, leading to a substantial increase in toughness[1]. The main areas of FRC applications are slabs on grade, tunnel linings, precast, and prestressed concrete products. Recently, elevated slabs of steel fibre-reinforced concrete (SFRC) have been successfully used where fibres provide the primary reinforcement[2,3]. A wide range of fibre-reinforced concrete systems including glass fibre-reinforced concrete (GFRC)[4], engineered cementitious composite (ECC)[5,6], slurry infiltrated concrete (SIFCON)[7,8], and high performance fibre reinforced concrete (HPFRC) [9,10] require better design guidelines. To standardise these materials, Naaman and Reinhardt[11] defined "strain-hardening" and "strain-softening" classifications based on tensile responses. Within the second category, additional terms of "deflection-hardening" and "deflection-softening" are defined to further classify the flexural response.

Despite the fact that FRC has been used in the construction industry for more than four decades, applications are still limited to a few market sectors. This is mainly due to the lack of standard guidelines for design procedures. To facilitate the design process, technical guidelines for FRC have been developed by RILEM committee TC162-TDF for SFRC [12,13,14,15,16] during the past 15 years. The committee proposed three-point bending test of a notched beam specimen for material characterisation. The elastically equivalent flexural strength at specific crack mount opening displacement (CMOD) is empirically related to the tensile stress-strain model. The compression response is described by a parabolic-rectangular stress strain model. The strain compatibility analysis of a layered beam cross section is required to determine the ultimate moment capacity. Similar to the RILEM, German guidelines for design of flexural members use the strain compatibility analysis to determine the moment capacity[17]. In the UK[18], the practice of FRC traditionally followed the Japanese Standard JCI-SF4 (1984)[19]; however, it has recently shifted towards the RILEM design methodology. The Italian guideline is also based on load-deflection curves deduced from flexural or direct tension test [20]. The current US design guidelines for flexural members are based on empirical equations of Swamy et al.[21 22]. Particular type of fibres and nature of concrete were not specified in the guidelines. Henager and Doherty[23] proposed a tensile stress block for SFRC that is comparable with the ultimate strength design of ACI 318-05[24].

This paper proposes a design methodology for strain-softening FRC and consists of two parts: design for ultimate strength and design for serviceability. The design procedures are based on theoretical derivations of Soranakom and Mobasher[25,26], in addition to ACI 318-05[24] and RILEM TC 162-TDF[16]. Topics include nominal moment capacity; minimum post crack tensile strength for flexural cracking; tensile strain limit; short term deflection calculations, and a conversion design chart to correlate traditional reinforced concrete and FRC systems.

A design example of one-way slab is presented to illustrate the use of equations in design of typical structural members.

STRAIN-SOFTENING FRC MODEL

Tensile and compressive response of strain-softening FRC such as steel and polymeric fibre-reinforced concrete (SFRC and PFRC) can be simplified to idealized stress strain models as shown in Fig. 1(a)&(b). In these materials the contribution of fibres is mostly apparent in the post peak tensile region, where the response is described by a decaying stress strain relationship. It is however possible to assume an average constant post crack tensile strength σ_p for the softening response, which can be correlated to the fibre volume fraction and their bond characteristics[21-23].

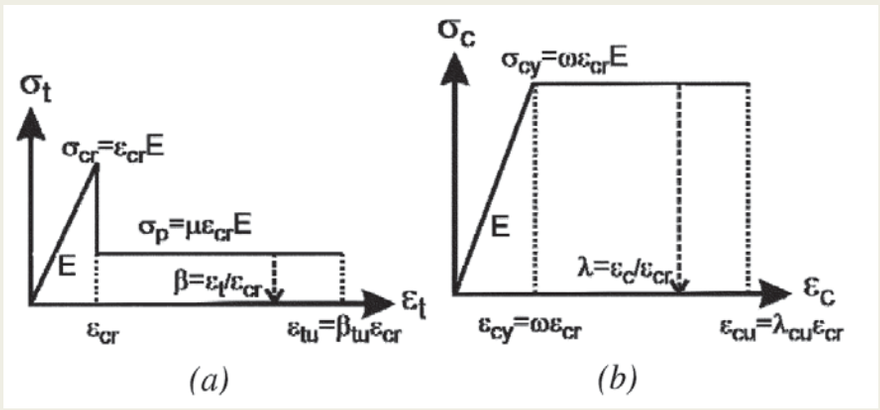

Fig 1 - Idealised material modelss for strain-softening fibre - reinforced cocrete: (A) Tension model; and (b) compression model

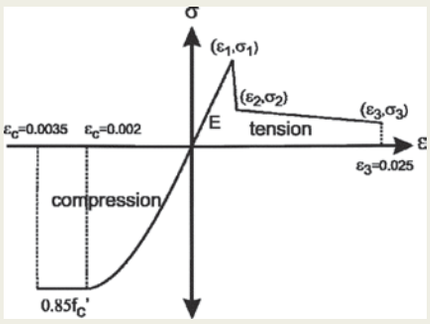

Fig 2 Idealised material models for strain-softening fibre-reinforced concrete: (a) tension model; and (b) compression model.

The following assumptions are made in the development of the material models: a) Young's modulus E for compression and tension are equal, b) tension model [Fig. 1(a)] consists of a linear stress strain response up to the cracking tensile strain ε_{cr}, followed by a constant post crack tensile strength $\sigma_p = \mu E\varepsilon_{cr}$ with parameter μ ($0 \le \mu \le 1$) representing the post crack strength as a fraction of the cracking tensile strength $\sigma_{cr} = E\varepsilon_{cr}$, and c) compression model defined by an elastic perfectly plastic model [Fig. 1(b)] using a yield compressive strain $\varepsilon_{cy} = \omega\varepsilon_{cr}$ with a parameter ω ($\omega \ge 1$) representing the compressive to cracking tensile strain ratio.

Study of material parameters[25] reveals that the ultimate moment capacity of FRC is significantly affected by the normalised post crack tensile strength parameter m while less sensitive to the compressive to tensile strength ratio w. In order to minimize the number of material parameters, the tensile strength and Young's modulus are assumed to be marginally affected by fibre type and content and conservatively estimated by the relationship governing normal concrete using ACI-318 Sec. 11.2 and Sec. 8.5.1, respectively.

$$\sigma_{cr} = E\varepsilon_{cr} = 0.56\sqrt{f_c'} \quad \text{(MPa)}$$
$$\text{(or } = 6.7\sqrt{f_c'} \quad \text{(psi))} \qquad (1)$$

$$E = 4{,}733\sqrt{f_c'} \quad \text{(MPa)}$$
$$\text{(or } = 57{,}000\sqrt{f_c'} \quad \text{(psi))} \qquad (2)$$

where f_c' is the ultimate uniaxial cylinder compressive strength. First crack tensile strain for FRC can be calculated assuming Hooke's law as:

$$\varepsilon_{cr} = \frac{\sigma_{cr}}{E} = \frac{0.56\sqrt{f_c'}}{4733\sqrt{f_c'}} = \frac{6.7\sqrt{f_c'}}{57000\sqrt{f_c'}} = 118\ \mu\text{str} \qquad (3)$$

According to the RILEM model[16] shown in Fig. 2, the ultimate tensile strain ε_3 is defined as 0.025. The ultimate compressive strain ε_{cu} is limited to 0.0035, which is the lower bound value of typical SFRC[27,28] ,and the yield compressive strength for FRC is adopted as:

$$\sigma_{cy} = 0.85f_c' \quad \text{(MPa and psi)} \qquad (4)$$

The two normalised parameters used in the material models [Fig. 1(a)&(b)] are summarised as follows:

$$\mu = \frac{\sigma_p}{E\varepsilon_{cr}} = \frac{\sigma_p}{\sigma_{cr}} \qquad (5)$$

$$\omega = \frac{\varepsilon_{cy}}{\varepsilon_{cr}} = \frac{\sigma_{cy}}{E\varepsilon_{cr}} = \frac{\sigma_{cy}}{\sigma_{cr}} = 1.52\sqrt{f_c'} \quad \text{(SIunit)}$$
$$\text{(or } 0.127\sqrt{f_c'} \quad \text{(US customary unit))} \qquad (6)$$

Note that the coefficients 1.52 and 0.127 used in Eq. (6) are for f_c' expressed in MPa and psi, respectively. Equation (6) implies that the normalised yield compressive strain ω is also a compressive to tensile strength ratio.

Research significance of reinforced concrete

The proposed design guideline provides computational efficiency over the commonly used strain compatibility analysis of a layered beam in determining moment capacity of FRC members.

The closed form equations and guidelines are compatible with the ACI-318 design method procedures while allowing deflection and serviceability criteria to be calculated, based on fundamentals of structural mechanics.

These computations allow engineers to reliably design and compare the overall performance of conventional reinforced concrete system and FRC.

Thus, these terms can be used interchangeably. For typical f_c' between 20 and 65 MPa, ω varies between 6.8 and 12.8. The tensile and compressive responses terminate at the normalised ultimate tensile strain b_{tu} and compressive strain λ_{cu} respectively.

$$\beta_{tu} = \frac{\varepsilon_{tu}}{\varepsilon_{cr}} = \frac{0.025}{118\times10^{-6}} \approx 212 \quad (7)$$

$$\lambda_{cu} = \frac{\varepsilon_{cu}}{\varepsilon_{cr}} = \frac{0.0035}{118\times10^{-6}} \approx 30 \quad (8)$$

Note that the terms β and λ without subscript refer to normalised tensile strain ($\varepsilon_t / \varepsilon_{cr}$) and compressive strain ($\varepsilon_c / \varepsilon_{cr}$), respectively and are functions of imposed curvature on a section.

Moment curvature response

For a rectangular section, the derivations for neutral axis depth ratio *k*, normalised moment *m*, and normalised curvature ϕ are described in an earlier publication[25]. Fig. 3 shows 3 ranges of applied top compressive strain $0 \le \varepsilon_c \le \varepsilon_{cr}$, $\varepsilon_{cr} \le \varepsilon_c \le \varepsilon_{cy}$ and $\varepsilon_{cy} \le \varepsilon_c \le \varepsilon_{cu}$ or in dimensionless form $0 \le \lambda \le 1$, $1 \le \lambda \le \omega$ and $\omega \le \lambda \le \lambda_{cu}$.

The location of neutral axis parameter *k* is derived by solving the equilibrium of internal forces. The moment was computed from taking the force about the neutral axis, while the curvature is obtained by dividing top compressive strain with the depth of neutral axis. The corresponding closed form solutions for normalised neutral axis, moment and curvature (*k*, *m*, ϕ) are presented in Table 1. Using these expressions, the moment *M* and curvature Φ represented in terms of their first cracking values (M_{cr} and Φ_{cr}) are defined as:

$$M = mM_{cr}; \quad M_{cr} = \frac{\sigma_{cr} b h^2}{6} \quad (9)$$

Range	*k*	*m*	ϕ
$0 \le \lambda \le 1$	$\frac{1}{2}$	$\frac{\lambda}{2k}$	$\frac{\lambda}{2k}$
$1 \le \lambda \le \omega$	$\frac{2\mu\lambda}{\lambda^2+2\mu(\lambda+1)-1}$	$\frac{(2\lambda^3+3\mu\lambda^2-3\mu+2)k^2}{\lambda^2}-3\mu(2k-1)$	
$\omega \le \lambda \le \lambda_{cu}$	$\frac{2\mu\lambda}{-\omega^2+2\lambda(\omega+\mu)+2\mu-1}$	$\frac{(3\omega\lambda^2-\omega^3+3\mu\lambda^2-3\mu+2)k^2}{\lambda^2}-3\mu(2k-1)$	

Table 1-Neutral axis depth ratio and normalised moment curvature expression for three ranges of applied normalised top comprehensive strain λ.

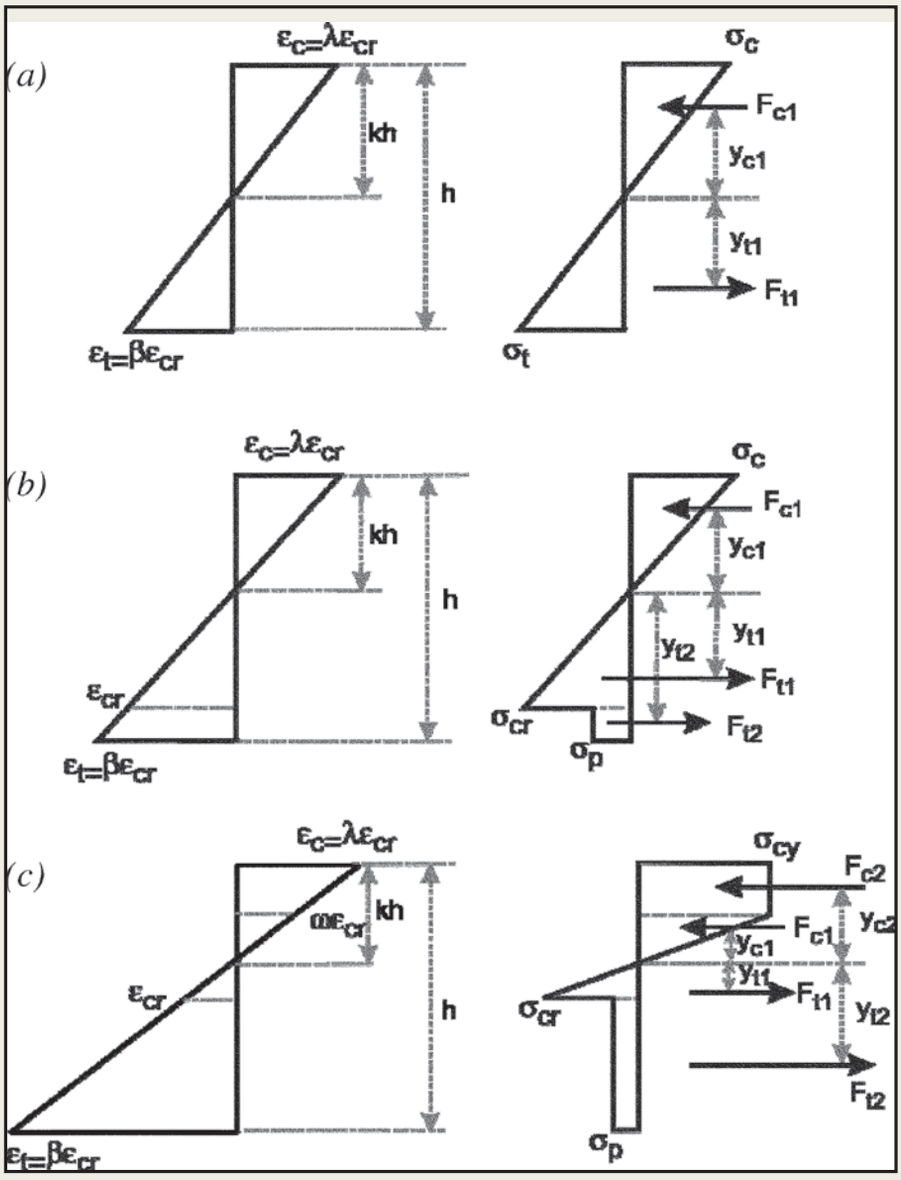

Figure 3-Stress-strain diagram at three ranges of normalised top comprehensive strain λ:(a) elastic for comprehension and tension (0 < λ ≤); (b) elastic for comprehension but nonlinear for tension (1 < λ ≤ω); (c) plastic for compression and nonlinear for tension (λ>ω).

$$\Phi = \phi\,\Phi_{cr}; \quad \Phi_{cr} = \frac{2\varepsilon_{cr}}{h} \quad (10)$$

where *b* and *h* are width and height of beam, respectively.

The moment capacity at ultimate compressive strain ($\lambda = \lambda_{cu}$) is very well approximated by the limit case of ($\lambda = \infty$). Using the expression for k in range 3 of Table 1, one obtains the neutral axis parameter at infinity k_∞.[25]

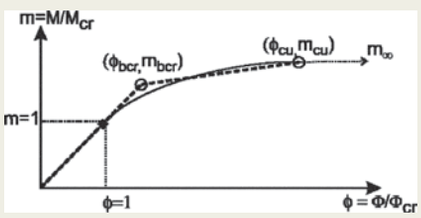

Figure 4-Normalised moment curvature response for strain-softening deflection-hardening material and it is simplified bilinear model.

ALLOWABLE TENSILE STRAIN

$$k_\infty = \frac{\mu}{\omega+\mu} \quad (11)$$

By substituting $k = k_\infty$ and $\lambda = \infty$ in the expression for m in range 3 of Table 1, the ultimate moment capacity, m_∞ is also obtained

$$m_\infty = \frac{3\omega\mu}{\omega+\mu} \quad (12)$$

BI-LINEAR MOMENT-CURVATURE DIAGRAM

For sufficiently high post peak tensile capacity, the flexural response of FRC shows no drop in moment capacity after cracking and is referred to as strain-softening deflection-hardening.

Fig. 4 shows a typical moment-curvature response for this class of material generated from Table 1. The smooth response can be approximated as a bilinear response using an optimization approach in the curve fitting.

The termination point of the bi-linear model was designated as m_{cu} and assumed to be equal to m_∞ given by Eq. (12). The intersection point is defined as the bilinear cracking point (ϕ_{bcr}, m_{bcr}) and is higher than the original cracking point (ϕ_{cr}, m_{cr}). With the predetermined bi-linear cracking points from material database covering possible range of FRC,[25,29] a linear regression equation was established as:

$$m_{bcr} = 0.743 m_{cu} + 0.174$$
$$\text{and} \quad \phi_{bcr} = m_{bcr} \quad (13)$$

The curvature at the ultimate compressive strain ϕ_{cu} can be determined by substituting a relatively large λ_{cu} value in the expression for k and ϕ in range 3 presented in Table 1. For example a simplified expression for ϕ_{cu} at λ_{cu} =30 is:

$$\phi_{cu} = \frac{-\omega^2 + 60\omega + 62\mu - 1}{4\mu} \quad (14)$$

The bilinear model can be used to obtain the curvature distribution according to a given moment profile. The slope in the elastic part is $\phi_{br}/m_{br} = 1$ while the slope in the post crack region is

$$\theta_{pcr} = \frac{\phi_{cu} - \phi_{bcr}}{m_{cu} - m_{bcr}} \quad (15)$$

Finally, the normalised curvature-moment relationship can be expressed as:

$$\phi = \begin{cases} m & \text{for } 0 < m \le m_{bcr} \\ \phi_{bcr} + \theta_{pcr}(m - m_{bcr}) & \text{for } m > m_{bcr} \end{cases} \quad (16)$$

For sufficiently high fibre volume fractions and a good bond property, the ultimate moment capacity of the strain-softening FRC can be as high as 2.6 times the first cracking moment[25]. There may however be a need to design based on a limit to the allowable tensile strain and crack width.

Since many deflection-hardening FRCs show multiple cracking, the nominal tensile strain averaged from several cracks spaced apart is proposed as the serviceability criterion. This section only addresses the effect of lower and upper bounds of the allowable tensile limit and their effect on service moments.

From the linear strain diagrams in the post crack ranges [Fig. 3(b)&(c)], the relationship between normalised allowable tensile strain β_a and the corresponding normalised compressive stain λ_a at a balanced condition can be written as:

$$\frac{\lambda_a \varepsilon_{cr}}{kh} = \frac{\beta_a \varepsilon_{cr}}{h - kh} \quad (17)$$

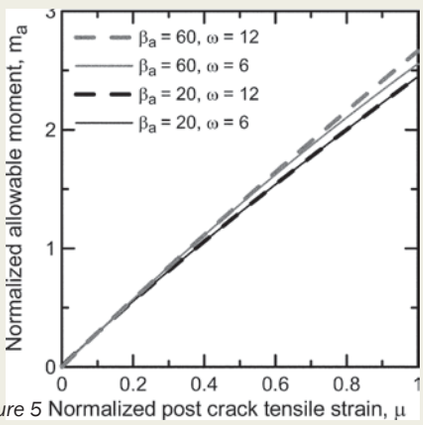

Figure 5 Normalized post crack tensile strain, μ

Table 3-Steel fibre reinforced concrete parameters for RILEM model.

Mixture	W_f, kg/m^3 (lb/yd^3)	E, MPa (psi)	f'_c, MPa (psi)	σ_1, MPa (psi)	σ_2, MPa (psi)	σ_3, MPa (psi)	ε_1, %	ε_2, %	ε_3, %
NSC	25 (42)	31,854 (4.62E + 06)	30.2 (4380)	3.5 (508)	1.1 (160)	0.8 (116)	0.011	0.21	25
NSC	50 (84)	30,564 (4.43E + 06)	26.6 (3858)	4.2 (609)	2.0 (290)	1.2 (174)	0.014	0.24	25
HSC	60 (101)	38,411 (5.57E + 06)	52.9 (7673)	6.2 (899)	3.1 (450)	3.1 (450)	0.016	0.26	25

Note: Strain at compressive yield stress $\varepsilon_{cy} = 0.133\%$, and ultimate compressive strain $\varepsilon_{cu} = 0.35\%$ for all mixtures.

Table 2-Normalised allowable moment.

Range		$\omega = 6$	$\omega = 12$
m_{2a} $1 \le \lambda \le \omega$	$\beta_a = 20$	$\frac{76\mu\sqrt{38\mu+1} + 2\sqrt{38\mu+1} + 1197\mu + 2}{(20 + \sqrt{38\mu+1})^2}$	
	$\beta_a = 60$	$\frac{236\mu\sqrt{118\mu+1} + 2\sqrt{118\mu+1} + 10{,}797\mu + 2}{(60 + \sqrt{118\mu+1})^2}$	
m_{3a} $\omega \le \lambda \le \lambda_{cu}$	$\beta_a = 20$	$\frac{18(1444\mu^2 + 12{,}388\mu - 343)}{(277 + 38\mu)^2}$	$\frac{36(1444\mu^2 + 30{,}172\mu - 6591)}{(625 + 38\mu)^2}$
	$\beta_a = 60$	$\frac{18(13{,}924\mu^2 + 95{,}108\mu - 343)}{(757 + 118\mu)^2}$	$\frac{36(13{,}924\mu^2 + 206{,}972\mu - 6591)}{(1585 + 118\mu)^2}$

Equation (17) is solved in conjunction with the neutral axis parameter *k* defined in Table 1 for two possible ranges 2 or 3. This results in two possibilities of λ_a:

$$\lambda_a = \begin{cases} \sqrt{2\mu\beta_a - 2\mu + 1} & \text{for } \beta_a \le \beta_{crit} \\ \dfrac{2\mu\beta_a - 2\mu + \omega^2 + 1}{2\omega} & \text{for } \beta_a > \beta_{crit} \end{cases} \quad (18)$$

$$\beta_{crit} = \frac{\omega^2 + 2\mu - 1}{2\mu} \quad (19)$$

where β_{crit} is the critical tensile strain. When $\beta_a \le \beta_{crit}$ the parameter λ_a will be in between 1 and ω (range 2) and when $\beta_a > \beta_{crit}$' the parameter λ_a will be greater than β_a range 3.

Two levels of normalised allowable tensile strain β_a = 20 and 60 (corresponding to 2360 and 7080 mstr for the cracking strain of 118 mstr defined in Eq. (3)) and the lower and upper bound compressive tensile strength ratio ω = 6 and 12 are evaluated. The closed form solutions for the allowable moments corresponding the combination of these β_a and ω can be derived by first substituting the values in Eq. (18), then substituting the obtained λ_a and/or ω in the expressions for *k* and *m* in range 2 and 3 in Table 3. The final form of allowable moments in range 2 or 3 (m_{2a} and m_{3a}) are presented in Table 2 depending on the value of β_a compared to β_{crit} as shown in Eq. (19).

Fig. 5 presents normalised allowable moment for post crack tensile strain β in the range of 0.0 - 1.0. The increase in allowable tensile strain β_a from 20 to 60 for each level of w slightly increases the allowable moment, with the maximum difference of only 8.8% at μ = 1.0. Thus, use of lower bound value β_a= 20 as a tensile strain criterion is reasonably safe for preventing excessive cracking while the moment capacity is slightly reduced. Note that at β_a= 20, the allowable moment is insensitive to changes of ω between 6 and 12, while at β_a = 60, only small differences are observed.

Based on this simplification, a conservative case of β_a = 20 and ω = 6 as presented in Table 2 is proposed as a tensile strain criterion and summarised as: (see top of page)

$$m_a = \begin{cases} \dfrac{76\mu\sqrt{38\mu+1} + 2\sqrt{38\mu+1} + 1197\mu + 2}{\left(20 + \sqrt{38\mu+1}\right)^2} & \text{for } \beta_a = 20 \le \dfrac{35+2\mu}{2\mu} \\ \dfrac{18\left(1444\mu^2 + 12388\mu - 343\right)}{(277 + 38\mu)^2} & \text{for } \beta_a = 20 > \dfrac{35+2\mu}{2\mu} \end{cases} \quad (20)$$

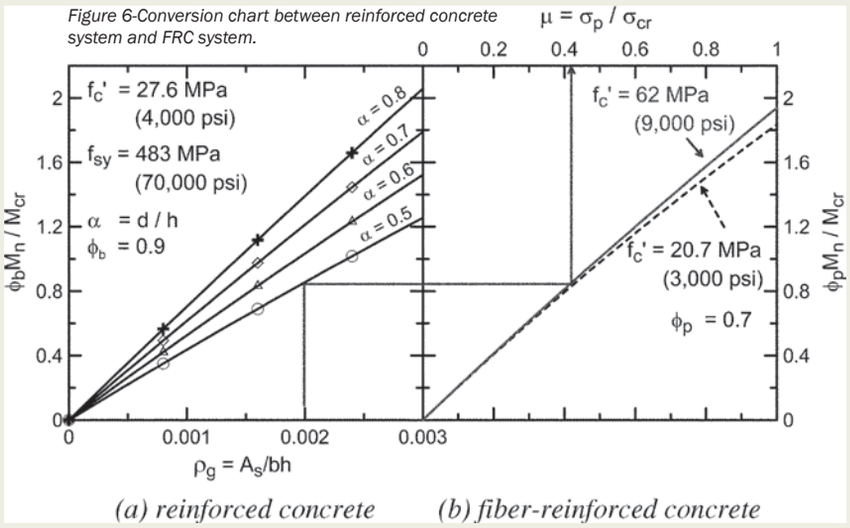

Figure 6-Conversion chart between reinforced concrete system and FRC system.

ULTIMATE MOMENT CAPACITY

Load and resistance factor design (LRFD) is based on the reduced nominal moment capacity $\phi_p M_n$ exceeding the ultimate factored moment M_u that is determined by linear elastic analysis and load coefficients in accordance to ACI 318-05 Sec 9.2. The reduction factor ϕ_p addresses the uncertainty of using post crack tensile strength in predicting ultimate moment capacity. Based on the statistical analysis of limited test data[29] a value ϕ_p = 0.7 was used in this study. The nominal moment capacity M_n can be obtained by using Eqs. (9)&(12) with the reduction factor: Alternatively, the nominal moment capacity can be expressed as a function of post crack tensile strength m and compressive strength ϕ_c' by substituting Eq. (6) in (21).

The post crack tensile strength necessary to carry the ultimate moment can be obtained from Eq. (22) as:

Strain-softening FRC has therefore a moment capacity that ranges between 1.0 and 2.6 times the cracking moment (Fig. 5); therefore, it is suitable for slab applications where internal moment is relatively low compared to the cracking moment and shear is generally not critical.

For higher internal moment such as beams in structure, the use of fibres may not be sufficient and require additional rebar to increase the capacity.

The design of this flexural member is presented in reference[29] while shear capacity of using fibre-reinforced concrete can be found in literature[30,31].

$$\phi_p M_n = \phi_p m_\infty M_{cr} = \frac{3\omega\mu}{\omega+\mu}\phi_p M_{cr} \ge M_u \quad (21)$$

$$\phi_p M_n = \left[\frac{6\mu\sqrt{f_c'}}{\xi\mu + 2\sqrt{f_c'}}\right]\phi_p M_{cr} \quad (\xi=1.32 \text{ for } f_c' \text{ in MPa, } \xi=15.8 \text{ for } f_c' \text{ in psi}) \quad (22)$$

$$\mu = \frac{2M_u\sqrt{f_c'}}{6\phi_p M_{cr}\sqrt{f_c'} - \xi M_u} \quad (\xi=1.32 \text{ for } f_c' \text{ in MPa, } \xi=15.8 \text{ for } f_c' \text{ in psi}) \quad (23)$$

Minimum Post Crack Tensile Capacity for Flexure

To prevent a sudden drop of moment capacity after initial cracking, a minimum fibre dosage is required. The post crack tensile strength that maintains a load capacity equivalent to the cracking strength level ($M_n = M_{cr}$) is defined as m_{crit} and obtained by solving Eq. (21) with a reduction factor $\phi_p = 1$.

$$\mu_{crit} = \frac{\omega}{3\omega - 1} \qquad (24)$$

For typical FRC materials with compressive to tensile strain ratio ω ranging from 6 - 12 results in μ_{crit} = 0.353 - 0.343. A conservative value of $\mu_{mim,flex}$ = 0.35 therefore ensures post crack moment capacity higher than the first cracking moment.

Beam	Mixture	W_f, kg/m^3 (lb/yd^3)	L, m (ft)	S_{mid}, m (ft)	P_{max}, kN (kip)	$M_{u,exp}$, kN-m (kip-ft)	M_n, kN-m (kip-ft)
B1	NSC	25 (42)	1.0 (3.33)	0.2 (8.0)	26.7 (6.0)	5.34 (3.94)	4.25 (3.13)
B2	NSC	25 (42)	2.0 (6.67)	0.2 (8.0)	10.3 (2.3)	4.64 (3.42)	4.25 (3.13)
B3	NSC	50 (84)	1.0 (3.33)	0.2 (8.0)	27.1 (6.1)	5.42 (4.00)	7.44 (5.49)
B4	NSC	50 (84)	2.0 (6.67)	0.2 (8.0)	16.9 (3.8)	7.61 (5.61)	7.44 (5.49)
B5	HSC	60 (101)	1.0 (3.33)	0.2 (8.0)	63.4 (14.3)	12.68 (9.35)	11.71 (8.64)
B6	HSC	60 (101)	2.0 (6.67)	0.2 (8.0)	21.5 (4.8)	9.68 (7.14)	11.71 (8.64)

Table 5-Comparison of ultimate moment capacity obtained by test results and design equations.

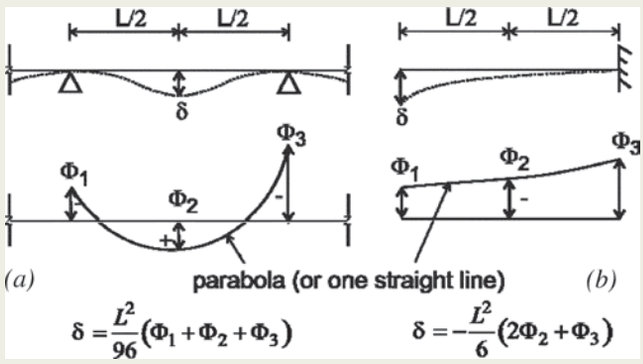

Figure 7-Geometric relationship between curvature and deflection[32,33].

Conversion Design Chart

An equivalent flexural FRC system can be substituted for minimum reinforcement in reinforced concrete structures. A conversion design chart is presented to help designers replace the reinforced concrete system with FRC system that has the same flexural capacity. The nominal moment capacity of a single reinforced concrete section can be determined by the compressive stress block concept (ACI Sec 10.2.7)

$$M_n = A_s f_y \left(d - \frac{a}{2} \right) \qquad (25)$$

where $a = A_s f_y / (0.85 f_c' b)$ is the depth of compressive stress block, $A_s = \rho_g bh$ is the area of tensile steel, ρ_g is the reinforcement ratio per gross section bh, and a is the normalised effective depth (d/h). The reduction factors ϕ_b = 0.9 and ϕ_p = 0.70 are used in the conversion chart to address the reliability of two reinforcing mechanisms. For any grade of steel and concrete strength, a conversion chart can be generated by Eqs. (22) and (25) as shown by Fig. 6.

The reinforcement ratio ρ_g together with the normalised effective depth *a* determine the moment capacity of the reinforced concrete system in Fig. 6(a) which can be transferred to the FRC chart to obtain normalised post crack tensile strength m in Fig. 6(b).

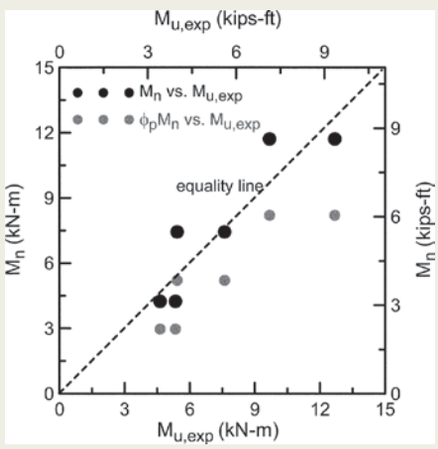

Figure 8-Predicted nominal moment capacity versus expreimental ultimate moment.

Table 4—Equivalent steel FRC parameters for the proposed model

Mixture	W_f, kg/m^3 (lb/yd^3)	σ_{cy}, MPa (psi)	σ_{cr}, MPa (psi)	σ_p, MPa (psi)	ω	μ	m_∞	b, m (in.)	h, m (in.)	M_{cr}, kN-m (kip-ft)	M_n, kN-m (kip-ft)
NSC	25 (42)	30.2 (4381)	3.5 (508)	1.1 (160)	8.63	0.31	0.91	0.2 (8.0)	0.2 (8.0)	4.67 (3.44)	4.25 (3.13)
NSC	50 (84)	26.6 (3858)	4.2 (609)	2.0 (290)	6.33	0.48	1.33	0.2 (8.0)	0.2 (8.0)	5.60 (4.13)	7.44 (5.49)
HSC	60 (101)	52.9 (7673)	6.2 (899)	3.1 (450)	8.53	0.50	1.42	0.2 (8.0)	0.2 (8.0)	8.27 (6.10)	11.71 (8.64)

Note: Strain at compressive yield stress ε_{cy} = 0.133%, and ultimate compressive strain ε_{cu} = 0.35 % for all mixtures.

Deflection calculation for serviceability

An important aspect of serviceability-based design is in accurate calculation of deflections under service load. The present approach can be used to compute the deflections by integration of the curvature along the beam length. Geometric relationship between curvature and deflection have been derived by Ghali[32,33]. The curvature distribution along the length can be arbitrary; however, a parabolic or linear shape result in accurate results while other shapes result in approximate values.

The sign convention for curvature is the same as the convention used for moments. Two typical cases of a simple beam (or continuous beam) and cantilever beam are presented in Fig. 7. The mid span deflection d of a simple (or continuous beam) can be computed by:

$$\delta = \frac{L^2}{96}(\Phi_1 + \Phi_2 + \Phi_3) \quad (26a)$$

The tip deflection of the cantilever beam can be computed by:

$$\delta = -\frac{L^2}{6}(2\Phi_2 + \Phi_3) \quad (26b)$$

where L is the span length, and Φ_1, Φ_2, and Φ_3 are the curvature at left end, centre, and right end, respectively. For short term deflection, the curvatures Φ_1 - Φ_3 due to moment at service loads can be estimated from Eqs. (10)&(16).

Model Prediction

Full scale beam tests from the Brite Eiram project BRPR-CT98-0813 "Test and design methods for steel fibre reinforced concrete" were used in the model verification[34]. The first set of the experimental programme studied the effects of concrete strength, fibre dosage, and span length on SFRC beams.

Two grades of normal strength concrete (NSC) and high strength concrete (HSC) were used. Normal strength concrete used the fibre type RC 65/60 BN at 25 and 50 kg/m^3 (42.1 and 84.3 lb/y^3) while HSC used fibre type RC 80/60 BP at 60 kg/m^3 (101.1 lb/y^3). Two span lengths of 1.0 and 2.0 m (3.33 and 6.67 ft) were used for the same cross section of 0.20 x 0.20 m (8 x 8 in). Two replicate samples were tested under four point bending for each span length while the spacing between the two point loads was kept constant at 0.2 m (8 in).

Material properties were characterized according to the RILEM model as shown in Fig. 2 and presented in Table 3. Key strength parameters used in the design were computed as shown in Table 4: $\sigma_{cy} = 0.85 f_c'$, $\sigma_{cr} = \sigma_1$, $\sigma_p = (\sigma_2 + \sigma_3)/2$. Using these definitions μ, ω, M_{cr}, and m_∞, can be calculated by Eqs. (5), (6), (9), and (12), respectively. Nominal moment capacity M_n can be calculated by Eq. (21) with $\phi_p = 1$. Note that Eq. (21) was used instead of (22) since $\omega = 0.85 f_c'/\sigma_1$ was obtained directly from Table 3. On the contrary, Eq. (22) ignores s_1 by assuming $\sigma_{cr} = 0.56 f_c'^{0.5}$ (or $6.7 f_c'^{0.5}$) and defines $\omega = 0.85 f_c'/\sigma_{cr} = 1.53 f_c'^{0.5}$ (or $0.127 f_c'^{0.5}$). Table 5 presents the average test results of two replicates of the six beams (B1-B6) series for three mixtures and two span lengths.

To compare the test results with the nominal moment capacity M_n, ultimate moment of the section $M_{u,exp}$ was calculated from the maximum experimental load P_{max}.

$$M_{u,exp} = \frac{P_{max}(L - S_{mid})}{4} \quad (27)$$

where L is the clear span and S_{mid} is the spacing between the load points defined earlier. The experimental capacity $M_{u,exp}$ was compared to the proposed nominal moment capacity M_n in Fig. 8 and they show good agreement with some variation. By using the recommended reduction factor ϕ_p of 0.7, the reduced moment capacity $\phi_p M_n$ is obtained well below the experimentally obtained values [29].

Design examples

The design procedure for FRC is best suited for thin structural applications such as slabs and wall systems since size effect is minimal and the applied moment is relatively low compared to the cracking moment.

An example is presented to demonstrate the design calculations for a one-way slab with a single span of 3.5 m (11.67 ft) subjected to a uniformly distributed live load of 2.0 kN/m^2 (41.8 lb/ft^2) and superimposed dead load of 0.7 kN/m^2 (14.6 lb/ft^2). A point load of 4.0 kN/m (0.274 kips/ft) is applied at the centre. The design requires use of SFRC with a compressive strength ϕ_c' of 45 MPa (6531 psi) and unit weight of 24 kN/m^3 (153 lb/ft^3).

Ultimate moment capacity

The one-way slab is designed based on 1.0 m strip (3.33 ft). The self weight for an assumed thickness of 0.15 m (6 in) is:

$$w_{sw} = 0.15 \quad 24 = 3.6\ kN/m^2 \quad (75.2\ lb/ft^2)$$

The factored loads according to ACI Sec. 9.2.1 are

$$w_u = 1.2(3.6 + 0.7) + 1.6(2.0) = 8.36\ kN/m^2 \quad (174.6\ lb/ft^2)$$

$$P_u = 1.6(4.0) = 6.4\ kN/m \quad (0.439\ kips/ft)$$

The maximum moment at mid span due to the uniform and point loads

$$M_u = \frac{w_u L^2}{8} + \frac{P_u L}{4} = \frac{8.36 \quad 3.5^2}{8} + \frac{6.4 \quad 3.5}{4} = 18.4\ kN\text{-}m/m \quad (4.14\ kip\text{-}ft/ft)$$

Tensile strength and cracking moment are estimated by Eqs. (1)&(9), respectively.

$$\sigma_{cr} = 0.56\sqrt{45} = 3.75\ MPa \quad (544\ psi)$$

$$M_{cr} = \frac{\sigma_{cr} b h^2}{6} = \frac{(3.75 \times 10^3) \times 1.0 \times 0.15^2}{6} = 14.06\ kN\text{-}m/m \quad (3.16\ kips\text{-}ft/ft)$$

The required post crack tensile strength for the ultimate moment M_u by Eq. (23) is:

$$\mu = \frac{2M_u\sqrt{f_c'}}{6\phi_p M_{cr}\sqrt{f_c'} - \xi M_u}$$

$$= \frac{2 \times 18.4\sqrt{45}}{6 \times 0.7 \times 14.06\sqrt{45} - 1.32 \times 18.4} = 0.66$$

$$= 0.66$$

Check tensile strain limit

The post crack tensile strength is determined by Eq. (1), $\sigma_p = \mu\sigma_{cr} = 0.66 \times 3.75 = 2.48$ MPa(360 psi)

Since the allowable tensile strain $\beta_a = 20 > (35 + 2 \times 0.66) / (2 \times 0.66) = 27.5$ in Eq. (20), the allowable moment is calculated as:

$$m_a = \frac{18\left(1444\mu^2 + 12388\mu - 343\right)}{(277 + 38\mu)^2}$$

$$= \frac{18\left(1444\times 0.66^2 + 12388\times 0.66 - 343\right)}{(277 + 38\times 0.66)^2} = 1.67$$

Unfactored loads are used to calculate the moment at service condition at the mid span.

$$M_s = \frac{wL^2}{8} + \frac{PL}{4} = \frac{(3.6 + 0.7 + 2.0) \quad 3.5^2}{8} + \frac{4.0 \quad 3.5}{4} =$$

$$= 13.15 \text{ kN-m/m} \text{ (2.96 kips-ft/ft)}$$

The normalised moment at service load is

$$m_s = \frac{M_s}{M_{cr}} = \frac{13.15}{14.06} = 0.935 \quad < m_a = 1.67 \Rightarrow \text{“passed”}$$

Short term deflection

In order to calculate the deflection, the bilinear curvature-moment relationship is generated. The compressive to tensile strength ratio w computed by Eq. (6) is:

$$\omega = 1.52\sqrt{f'_c} = 1.52\sqrt{45} = 10.2$$

Two data points (ϕ_{br}, m_{br}) and (ϕ_{cu}, m_{cu}), and the slope θ_{pcr} in the post crack region can be determined by Eqs. (12)-(16).

$$m_{cu} = m_\infty = \frac{3\omega\mu}{\omega+\mu} = \frac{3\times 10.2\times 0.66}{10.2+0.66} = 1.86$$

$$\phi_{cu} = \frac{-\omega^2 + 60\omega + 62\mu - 1}{4\mu}$$

$$= \frac{-10.2^2 + 60\times 10.2 + 62\times 0.66 - 1}{4\times 0.66} = 207.5$$

$$m_{bcr} = 0.743 m_u + 0.174 = 0.743 \quad 1.86 + 0.174 =$$

$$= 1.56$$

$$\phi_{bcr} = m_{bcr} = 1.56$$

$$\theta_{pcr} = \frac{\phi_{cu} - \phi_{bcr}}{m_{cu} - m_{bcr}} = \frac{207.5 - 1.56}{1.86 - 1.56} = 686.5$$

For a simple beam case, the curvature at both ends (Φ_1 and Φ_3) are zero and the curvature at midspan Φ_2 is determined by Eqs. (10)&(16). Since m_s is less than m_{bcr} thus $\phi_2 = m_s$.

$$\Phi_2 = \phi_2\Phi_{cr} = m_s\frac{2\varepsilon_{cr}}{h} = 0.935\frac{2\times 118\times 10^{-6}}{150} =$$

$$= 1.471\times 10^{-6} \quad mm^{-1} \text{ (3.736 x } 10^{-5} \text{ in}^{-1}\text{)}$$

Finally, the mid span deflection of the beam is calculated by the geometric relationship between curvature and deflection defined in Eq. (29.1)

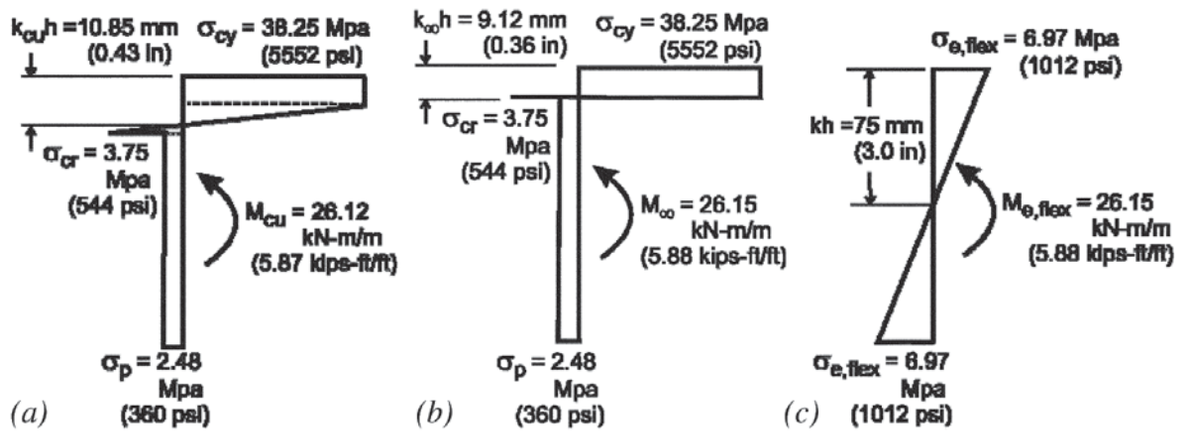

Fig. 9—Stress distribution at ultimate moment: (a) idealized material models at ultimate compressive strain; (b) idealized material models at infinite compressive strain; and (c) elastically equivalent flexural stress.

Short term deflection

$$\delta = \frac{L^2}{96}(\Phi_1 + \Phi_2 + \Phi_3) = \frac{3500^2}{96}\left(1.471\times10^{-6}\right)$$

$$= 0.188 \ mm \ (0.0074 \text{ in})$$

Note that in order to check the deflection limit for each application, long term effects such as creep and shrinkage must be taken into account. This aspect is beyond the scope of this paper.

Stress distributions

In order to demonstrate the differences between the present method and the commonly used elastically equivalent flexural strength $\sigma_{e,flex}$, stress distribution across the beam section at ultimate compressive strain and at infinite strain are compared with the elastic flexural stress. The neutral axis at ultimate compressive strain ε_{cu} of 0.0035, in addition to the ultimate moment are obtained by substituting λ_{cu} = 30 in the expressions for *k* and *m* in range 3 of Table 1.

$$k_{cu} = \frac{2\mu\lambda_{cu}}{-\omega^2 + 2\lambda_{cu}(\omega+\mu) + 2\mu - 1}$$

$$= \frac{2\times0.66\times30}{-10.2^2 + 2\times30(10.2+0.66) + 2\times0.66 - 1} = 0.0723$$

$$k_{cu}h = 0.0723 \quad 150 = 10.85 \ mm$$

$$m_{cu} = \frac{(3\omega\lambda_{cu}{}^2 - \omega^3 + 3\mu\lambda_{cu}{}^2 - 3\mu + 2)k_{cu}{}^2}{\lambda_{cu}{}^2} - 3\mu(2k_{cu} - 1)$$

$$= \frac{\left(3\times10.2\times30^2 - 10.2^3 + 3\times0.66\times30^2 - 3\times0.66 + 2\right)}{30^2}0.0723^2$$

$$- 3\times0.66(2\times0.0724 - 1)$$

$$= 1.858$$

$$M_{cu} = m_{cu}M_{cr} = 1.858 \quad 14.06 = 26.12 \ kN\text{-}m/m$$

$$(5.87 \text{ KIPS-FT/FT})$$

The neutral axis parameter and moment at infinite compressive strain are obtained by Eqs. (9), (11)&(12).

$$k_\infty h = \frac{\mu}{\omega+\mu}h = \frac{0.66}{10.2+0.66}\times150 = 9.12 \ mm \quad (0.36 \text{ in})$$

$$M_\infty = m_\infty M_{cr} = \frac{3\omega\mu}{\omega+\mu}M_{cr} = \frac{3\times10.2\times0.66}{10.2+0.66}\times14.06$$

$$= 26.15 \ kN\text{-}m/m \ (5.88 \text{ kips-ft/ft})$$

The elastically equivalent flexural strength corresponding to the nominal moment of 26.15 kN-m/m is determined by the flexure formula.

$$\sigma_{e,flex} = \frac{M_u c}{I} = \frac{(26.15\times10^3)\times0.15/2}{1.0\times0.15^3/12}$$

$$= 6.97 \text{ MPa} \qquad (1012 \text{ psi})$$

Stress distributions calculated by the three approaches are compared in Fig. 9. It can be seen that the post crack tensile strength between the idealized material models at ultimate compressive strain (ε_{cu} = 0.0035) and at infinity ($\varepsilon_{cu} = \infty$) are the same at σ_p = 2.48 MPa (360 psi). This level of post crack stress is much smaller than the elastically equivalent flexural strength $\sigma_{e,flex}$ of 6.97 MPa (1012 psi). On the other hand the compressive stress at ultimate strain and at infinity are the same at σ_{cy} = 38.25 MPa (5552 psi) which is much higher than $\sigma_{e,flex}$ of 6.97 MPa (1012 psi). This example points out the inadequacies of several inverse analysis techniques that have been used to obtain residual tensile capacity such as the average residual stress method (ASTM C 1399-04)[35] which report material strengths in terms of equivalent elastic values. Designers should be aware of the shortcomings of these methods and approaches that determine member capacity.

The neutral axis of the idealized model at ultimate compressive strain is slightly higher than the neutral axis at infinity. However, the moment capacities are quite close to one another (26.12 vs. 26.15 kN-m/m). This is due to the elastic stress regions near the neutral axis decreasing while the plastic tensile regions increase.

Acknowledgements

The authors acknowledge the National Science Foundation, programme 0324669-03, Dr P Balaguru, programme manager and Salt River Project for supporting this project.

Conclusions

A design guideline for strain-softening FRC is presented using closed form analytical equations that relate geometrical and material properties to moment and curvature capacity. Conservative reduction factors are introduced for using post crack tensile strength in design and a conversion design chart is proposed for developing FRC systems equivalent to traditional reinforced concretes.

The moment-curvature response for a strain-softening deflection-hardening FRC can be approximated by a bi-linear model while geometric relationship between curvature and deflection can be used for serviceability deflection checks.

REFERENCE

1. ACI (American Concrete Institute), "State-of-the-Art Report on Fibre-Reinforced Concrete," ACI 544.1R-82, 1982. pp. 21

2. Destrée, X., "Concrete Free Suspended Elevated Slabs Reinforced with Only Steel Fibres: Full Scale Testing Results and Conclusions – Design Examples', International Workshop on High Performance Fibre-Reinforced Cementitious Composites in Structural Applications, Honolulu, HI, RILEM Publications SARL, May 2005, pp. 287-294.

3. Soranakom, C.; Mobasher, B.; and Destrée, X., "Numerical Simulation of FRC Round Panel Tests and Full-Scale Elevated Slabs," ACI SP-248-3, Sept. 2007, pp. 31-40.

4. PCI Committee on Glass Fibre-Reinforced Concrete Panels, Recommended Practice for Glass Fibre Reinforced Concrete Panels, third edition, Precast/Prestressed Concrete Institute, 1993, 99 pp.

5. Maalej, M., and Li, V.C., "Flexural/Tensile-Strength Ratio in Engineered Cementitious Composites," Journal of Material in Civil Engineering, V.6, No. 4, Nov. 1994, pp. 513–528.

6. Li, V.C., "On Engineered Cementitious Composites (ECC): A Review of the Material and Its Applications," Journal of Advance Concrete Technology, V. 1, No. 3, Nov. 2003, pp. 215-230.

7. Krstulovic-Opara, N., and Malak, S. "Tensile Behaviour of Slurry Infiltrated Mat Concrete (SIMCON)," ACI Materials Journal, V. 94, No. 1, Jan.-Feb. 1997, pp. 39–46.

8. Bayasi, Z., and Zeng, J., "Flexural Behaviour of Slurry Infiltrated Mat Concrete (SIMCON)," Journal of Materials in Civil Engineering, V. 9, No. 4, Nov. 1997, pp. 194–199.

9. Chanvillard G., and Rigaud, S., "Complete Characterisation of Tensile Properties of Ductal UHPFRC according to the French Recommendations," Proceeding of the 4th International RILEM Workshop, High Performance Fibre-Reinforced Cement Composites (HPFRCC4), Ann Arbor, USA, Jun. 2003, 21-34.

10. Benson, S. D. P., Karihaloo, B. L., "CARDIFRC [registered trademark] -Development and Mechanical Properties. Part I: Development and workability," Magazine of Concrete Research, V. 57, No. 6, Aug. 2005, pp. 347-352.

11. Naaman, A. E., and Reinhardt H. W., "Proposed Classification of HPFRC Composites Based on Their Tensile Response," Materials and Structures, V. 39, No. 289, Jun. 2006, pp. 547–555.

12. Vandewalle, L. et al. "Test and Design Methods for Steel Fibre-Reinforced Concrete. Recommendations for Bending Test," Materials and Structures, V. 33, No. 225, Jan. 2000a, pp. 3-5.

13. Vandewalle, L. et al., "Test and Design Methods for Steel Fibre-Reinforced Concrete: Recommendations for σ-ε Design Method," Materials and Structures, V. 33, No. 226, Mar. 2000b, pp. 75-81.

14.Vandewalle, L. et al., "Design of Steel Fibre-Reinforced Concrete Using the s-w Method: Principle and Applications," Materials and Structures, V. 35, No. 249, Jun. 2002a, pp. 262-278.

15. Vandewalle, L. et al., "Test and Design Methods for Steel Fibre Reinforced Concrete - Final Recommendation," Materials and Structures, V. 35, No. 253, Nov. 2002b, pp. 579-582.

16. Vandewalle, L. et al. "Test and Design Methods for Steel Fibre Reinforced Concrete-s-e Design Method - Final Recommendation," Materials and Structures, V. 36, No. 262, Oct. 2003, pp. 560-567.

17.Teutsch, M., "German Guidelines on Steel Fibre Concrete," Proceeding of the North American/European Workshop on Advances in Fibre Reinforced Concrete, BEFIB 2004, Bergamo, Italy, Sept. 2004, pp. 23-28.

18. Barr B., and Lee, M.K., "FRC Guidelines in the UK, with Emphasis on SFRC in Floor Slabs," Proceeding of the North American/European Workshop on Advances in Fibre Reinforced Concrete, BEFIB 2004, Bergamo, Italy, Sept. 2004, pp. 29-38.

19. Japan Society of Civil Engineers JSCE-SF4., "Methods of Tests for Flexural Strength and Flexural Toughness of Steel Fibre Reinforced Concrete," Concrete Library International, Part III-2, 3, 1984, pp. 58-61.

20. di Prisco, M.; Toniolo, G.; Plizzari, G. A.; Cangiano, S.; and Failla, C., "Italian Guidelines on SFRC," Proceeding of the North American/European Workshop on Advances in Fiber Reinforced Concrete, BEFIB 2004, Bergamo, Italy, Sept. 2004, pp. 39–72.

21. Swamy, R.N.; Mangat, P.S.; and Rao, C.V.S.K., "The Mechanics of Fibre Reinforced Cement Matrices," Fiber Reinforced Concrete ACI SP-44, 1975, pp. 1-28.

22. Fischer, G. "Current U.S. Guidelines on Fibre Reinforced Concrete and Implementation in Structural Design," Proceeding of the North American/European Workshop on Advances in Fibre Reinforced Concrete, BEFIB 2004, Bergamo, Italy, Sept. 2004, pp. 13-22.

23. Henager, C.H., and Doherty, T.J., "Analysis of Reinforced Fibrous Concrete Beams," Proceedings, ASCE. V.12 ST-1, pp. 177-188.

24. ACI Committee 318, Building Code Requirements for Structural Concrete, ACI Manual of Concrete Practice, American Concrete Institute, Detroit, 2005.

25. Soranakom, C., and Mobasher, B., "Closed-Form Solutions for Flexural Response of Fibre-Reinforced Concrete Beams," Journal of Engineering Mechanics, V. 133, No. 8, Aug. 2007, pp. 933-941.

26. Soranakom, C., and Mobasher, B., "Development of Design Guidelines for Strain Softening Fibre Reinforced Concrete," 7th RILEM International Symposium on Fibre Reinforced Concrete, BEFIB 2008, Chennai (Madras), India, Sept. 2008, pp. 513-523.

27. Swamy R.N., Al-Ta'an S.A. "Deformation and Ultimate Strength in Flexural of Reinforced Concrete Beams Made with Steel Fibre Concrete," ACI Structural Journal, Vol. 78, No. 5, Sept. - Oct. 1981, pp. 395-405.

28. Hassoun M.N., Sahebjam K. "Plastic Hinge in Two-Span Reinforced Concrete Beams Containing Steel Fibres," Prc., Can. Soc. For Civ. Engrg. 1985, pp. 119-139.

29. Soranakom C., "Multi-Scale Modeling of Fibre and Fabric Reinforced Cement Based," Ph.D. Dissertation, Arizona State University, Tempe, USA, 2008.

30. Soranakom, C., and Mobasher, B., "Closed Form Solutions for Flexural Response of Hybrid Reinforced Concrete Beams: Part II - Experimental Verifications," ASCE Journal of Structural Engineering (Manuscript in review)

31. Kwak Y.-K., Eberhard, M.O., Kim, W.-S., and Kim, J., "Shear Strength of Steel Fibre-Reinforced Concrete Beams without Stirrups," ACI Structural Journal, V.99, No.4, July-August, 2002, pp. 530-538.

32 Parra-Montesinos, G., "Shear Strength of Beams with Deformed Steel Fibres-Evaluating an Alternative to Minimum Transverse Reinforcement," Concrete International, November, 2006, pp. 57-66.

33. Ghali, A., "Deflection of Reinforced Concrete Members: A Critical Review," ACI Structural Journal, V. 90, No. 4, July-August, 1993, pp. 364-373.

34. Ghali, A., and Favre, R., Concrete Structures: Stresses and Deformations, Chapman and Hall, London, 1986, 352 pp.

35. Dupont D., "Modelling and Experimental Validation of the Constitutive Law (s-e) and Cracking Behaviour of Steel Fibre Reinforced Concrete" Ph.D. Dissertation, Catholic, University of Leuven, Belgium, 2003.

36. ASTM C 1399-04, "Standard Tests Method for Obtaining Average Residual-Strength of Fibre-Reinforced Concrete," ASTM International, PA, 2004, 6 pp.

Peter Mokaba Stadium

A truly 'African' creation, the Peter Mokaba stadium in Polokwane is perhaps not the most audacious of stadia, but its wonder lies in the thinking behind the scenes.

Supported by giant 'trunk' structures which accommodate vertical circulation ramps and service cores, its structure embodies the spirit of Africa with an unmistakably iconic baobab design.

Its massive roof plane is gathered together at each corner in tree-like pleats to produce both rich cultural and historic significance.

Named after a renowned figure of the struggle for South Africa's emancipation against the apartheid regime, it's bleachers will be one of ten host venues for an estimated 3,5 million people during the FIFA World Cup.

Built next to the old Peter Mokaba Stadium, the structure is situated approximately 3 km from the city centre. The venue in the Limpopo Province has the capacity to seat 45 000.

Aurecon played a key role in the consortium responsible for the design of the stadium. Built on behalf of Polokwane Municipality by the WBHO/Paul JV as principal contractor, Aurecon provided full engineering disciplines, including civil, structural, geotechnical, electronic, HVAC and fire services.

Designed by AFL Architects, in JV with Prism, the stadium was the last to receive the go ahead in terms of construction. Its design feature simplified construction, ensuring completion in just two and a half years.

"Ultimately, our job was to save the client time, money and effort on the journey to meeting the very tight deadlines for stadium construction," says Aurecon Project Director, Stoffel Mentz. The overall design made use of modular concrete elements that were repeated throughout, which meant casting was simplified and could be done at high speed after the contractor had perfected the first few casts.

The casting of key elements together, such as Y-columns and raker beams for the upper terrace as a single element, reduced casting time considerably. In addition to the four identical 'baobab' structures, the lower tiers of all the stands, as well as the upper tiers are virtually identical.

The stands consist of reinforced concrete frames with raked concrete beams on the seating side to support the precast concrete seating elements. The same modular principle is evident in the roof structure which can easily be adapted to suit the differing needs for the stadium through simply removing and adding different pieces of the overhead structure.

The stadium's primary truss, a 175m triangular structural steel truss, presented a major engineering challenge in terms of both erection and the need for precise prediction and calculations. The behaviour of the truss varied according to differing weather conditions, and even a slight mis-calculation would mean the two ends wouldn't meet in the middle when hoisted. "It is immensely satisfying when design analysis and modelling come together to produce technical success," says Mentz.

The stadium was initially designed to accommodate a roof over all the stands – this was cut back to a single roof over the western stand which is a minimum requirement of FIFA.

The structure was designed such that a roof can also be installed over the eastern stand in future.

The total volume of in-situ cast concrete is approximately 60,000 m^3 and the total tonnage of reinforcement used is approximately 7,500 tons. The total volume of precast concrete (seating elements and vomitories) is approximately 6 500 m^3 and reinforcement used is approximately 780 tons. Total area covered by paving is approximately 120 000 m^2.

Low – density concrete

Low-density concrete is used for thermal insulation, for low density screeds and for low density back-fill to utility trenches or other excavations. It has also been used in cast-in place building systems, and pre-cast walling systems where it may perform a limited structural function.

There are three types of low-density concrete mix currently available in South Africa. Cement, light-weight aggregate, sand, water and admixtures. There's a mix of cement, fine sand and foaming agents, or no-fines concrete mixtures - where most, if not all, of the sand is omitted from the mix.

The three types of light-weight aggregate mixes that are generally available include: polystyrene beads and chips; exfoliated vermiculite from Mandoval Vermiculite, Gauteng, and perlite, available from Pratley. These aggregates are typically batched by volume, as errors can occur when batching mass, because the materials have very low bulk densities.

Typically they are supplied in 100 litre bags and the usual mix is one bag of cement to one bag of light-weight aggregate, ie 1:3 by volume. Sand may be added to increase the density and strength of the concrete and it also helps with the mixing process. Often up to one volume of sand is added. Leaner mixes (around 1:6) are used for mixes at the lower end of the density range. Admixtures may also be used. Air-entrainers are useful, as are pump-aids, to prevent the light-weight aggregate from floating out of the mix. Teepol has also been used successfully. Batching should be done in a wind-free area as the aggregates tend to blow around. Mixing can be done in drum-mixers but pan-mixers give better results.

The concrete is placed in the normal way but does not respond well to internal vibration. Compaction should be carried out with surface, form, or table vibrators. Early and thorough curing is important as these concretes have high drying shrinkage. Vermiculite concretes have very high water requirements and take a long time to dry out, after curing.

Densities as low as 400 kg/m^3 are achievable and range up to 900 kg/m^3.

Strength varies inversely with density and ranges from less than 1 up to 5 MPa. This type of concrete is not suitable for traffic areas and the surface must be protected if the concrete is to take any traffic flow.

Foamed concrete

Foamed concrete is made by diluting a concentrated foaming agent and passing it through a foam generator. The foam is poured into the mixer containing the sand-cement mortar and the concrete is mixed. Mortar proportions vary from 2 sand 1 cement to 1 sand 1 cement depending on density required. Densities vary from 400 to 1600 kg/m^3 and strengths from 1 to 10 MPa. Again, this type of concrete is not suitable for traffic and the surface must be protected if it is to be used for traffic.

Typical applications for this type of concrete are insulating roof screeds, and back-filling of trenches, mine shafts, old underground tanks etc. Mixes are flowable and able to be pumped.

No-fines concrete

Typically the mixes are in the region of 8 to 10 parts of single-sized stone to 1 part cement by volume 19-mm stone is normally used but smaller stone may also be utilised. Up to one part of fine sand may be added to the mix to increase the contact between the stone particles. The amount of water added is critical - too little water and the paste will not coat the stone, and too much water makes the paste run off the stone. No-fines concrete has a density of around 1600 kg/m^3 depending on the compacted bulk density of the stone being used. This type of concrete is ideal for drainage layers, soil stabilisation and porous dams.

No-fines concrete has excellent insulating properties and very little capillarity which makes it ideal for cast-in-place walling for houses. It is easy to render and because the walls are porous (behind the plaster) they are self-draining. The unconfined compressive strength of no-fines concrete is of the order of 3 to 5 MPa.

For further reading refer to:

1, Fulton's Concrete Technology, 8th ed, 2001, pp287 - 292

2. Technical Information Pamphlet No 110A, "Low Density Concrete, Polystyrene Bead Concrete", Cement and Concrete Institute, 1981

3) "Foamed Concrete", leaflet, Cement and Concrete Institute.

4) PPC Tip 24

William Nicol Bridge gets a lift

The widening of the William Nicol Bridge which crosses the N1 highway is just one of the many projects being undertaken by the Gauteng Freeway Improvement Project (GFIP) at present.

In total four portions of new bridge deck - on and off ramps, northbound and south bound - are to be lifted into place, being supported on its abutment by a column founded in the central median. Each portion is cast adjacent to its corresponding abutment to ensure that the deck curvature is exactly the same as its abutment.

This method of construction ensures that the N1 highway remains open during the bridge widening except for two days (for north bound and south bound traffic) when the deck sections are placed.

Each deck section has a mass of 100t and a 600t capacity crane is needed to lift and place each section. The placement is a precision operation requiring the deck to be perfectly level when positioned on the abutment and its supporting column. It can be seen that the design of the deck incorporates 'chambers' which, apart from combining strength with minimum weight, also has the added advantage of being able to be used to balance and level the deck, after being filled with water. Such was the precision of the lifting contractor, this operation was not necessary for the first two lifts.

The remaining southbound on and off ramp decks will be positioned during the coming months when work on the southbound abutments is completed. SSI Engineers and Environmental Consultants are involved in three work packages on the GFIP, the N1 Buccleuch to 14th Avenue, N3 Buccleuch to Gilloolys interchange and the N12 Gilloolys to Griffiths Road interchange. SSI is a multi-disciplinary consultancy.

The company's services cover the complete spectrum of lifecycle needs within the sectors of transport, water, environmental, energy and resources, buildings and structures and project and construction management.

The team of 900 operates in 20 major centres in the Southern hemisphere. Its majority shareholder is the DHV Group, one of Europe's leading engineering companies.

For further information please email robinh@ssi.co.za or visit the web site on www.ssi-dhv.com

Inland update

John Sheath

The Inland Branch held its Annual General Meeting in Midrand, Gauteng on the 4th of March. Chairman, John Sheath reported that despite a very difficult year in the industry, 2009 had been very successful for the inland branch. The mini-seminars, site visit to Gillooly's Interchange and the Annual Boat Race had all attracted record attendances.

Sheath thanked the various local sponsors for their generosity and support over the past year. He reminded members that without sponsors for the various events, at best, events would have cost the Branch a lot more, and at worst, would not have taken place at all.

The Branch's efforts to increase Company membership during 2009 had been moderately successful.

However, he says that this effort will continue during the year and urged companies to seriously consider Company Membership.Office Bearers for 2010 were confirmed: Chair – John Sheath, Vice-Chair – Johan van Wyk, Treasurer – Trevor Sawyer, Secretary – Bernice Baxter. In addition, six Committee Members have been elected: Hanlie Turner, Colin Kalis, Hannes Engelbrecht, Natalie Johnson, Michelle FIck, and Donovan Leach.

The AGM was followed by an excellent presentation by Bryan Perrie, Managing Director of the Cement and Concrete Institute. His talk "Concrete – it's greener than you think," covered preliminary results of research work commissioned by the institute into the carbon footprint of all constituents of concrete (eg cement, aggregate, extender, admixture, rebar and water) and also concrete itself. Using Cement as Base = 100 he was able to provide the audience with the relative carbon emission of all the constituent materials used in concrete.

According to Perrie, a holistic approach has been taken into establishing just how green concrete is and the final results of the work will be made public in the not too distant future.

The meeting concluded with refreshments kindly sponsored by the Cement and Concrete Institute.

ACM 2009


Dr Billy Boshoff, Prof VC Li, Prof F Wittmann, Dr WP Boshoff, Prof J van Mier, F Bain, Prof E Kearsley, Prof S Shah and Prof G van Zijl.

During November 2009 the CSSA, together with Stellenbosch University and supported by the Cement and Concrete Institute, organised the International Conference on Advanced Concrete Materials. It was held at the Wallenburg Conference Venue in Stellenbosch. Forty papers were delivered by international experts in the field of advanced concrete materials. The topics varied from nano-technology to bendable concrete. The event was well supported by the local industry and over 140 delegates attended the sessions. All the papers are available from the society's head office. The conference banquet was held at L'Avenir, a wine farm close to Stellenbosch and the guests were treated to great wines of the region.

The event was supported by Pretoria Portland Cement, BASF Construction Chemicals and Mapei. Lastly the organising committee made the first International Conference on Advanced Concrete Materials a highly successful event.

Company Membership Details

Platinum	Principal Member	Address	Tel No	Fax No
Lafarge Industries SA (Pty) Ltd	Mr D Miles	PO Box 11373 Silverlakes Pretoria 0054	011 257 3100	011 257 3038
AfriSam SA (Pty) Ltd	Mr M McDonald	PO Box 15 Roodepoort 1725	011 758 6000	011 670 5166

Gold	Principal Member	Address	Tel No	Fax No
NPC-Cimpor (Pty) Ltd	Mr P Strauss	PO Box 15245 Bellair 4006	031 450 4411	086 535 2772
Sika (Pty) Ltd	Mr P Adams	PO Box 15408 Westmead 3608	031 792 6500	031 700 1760
BKS Engineering & Mangement (Pty) Ltd	Mr PD Ronné	PO Box 112 Bellville 7535	021 950 7500	021 950 7502

Silver	Principal Member	Address	Tel No	Fax No
Cement & Concrete Institute	Mr B Perrie	PO Box 168 Halfway House 1685	011 315 0300	011 315 0584
MAPEI SA (Pty) Ltd	Mr C van der Merwe	PO Box 365 Brakpan 1540	011 876 5336	011 876 5160
Ash Resources (Pty) Ltd	Mr G Smith	PO Box 3017 Randburg 2025	011 886 2200	011 886 6140
Chryso SA (Pty) Ltd	Mr NS Seymore	Postnet Suite 59 Private Bag X1 East Rand 1462	011 395 9700	011 397 6644

Bronze	Principal Member	Address	Tel No	Fax No
Shukuma Flooring (Pty) Ltd	Mr A Stücki	PO Box 15552 Emerald Hill 6000	041 372 1933	041 372 1944
Lategan & Bouer Engineers	Mr K Lategan	PO Box 1251 Secunda 2302	017 634 4150	017 634 4188
Scribante Concrete (Pty) Ltd	Mr S Scribante	PO Box 2179 North End 6056	041 484 7211	041 484 6231
Quickslab (Pty) Ltd	Mr J Coetzee	PO Box 9 Brackenfell 7560	021 982 1490	021 982 1492
Empa Structures CC	Mr CA Bain	PO Box 3846 Durbanville 7551	021 988 8840	021 988 8750
Doka South Africa (Pty) Ltd	Mr U Meyer	PO Box 8337 Halfway House 1685	011 310 9709	011 310 9711
Jeffares & Green (Pty) Ltd	Mr CJ Meintjies	PO Box 13009 Cascades 3202	033 347 1841	033 347 1845
Verni Speciality Construction Products (Pty) Ltd	Mr VP Botha	PO Box 75393 Garden View 2047	086 118 3764	086 128 3764
Group 5 KZN	Mr G Chambers	PO Box 201219 Durban North 4019	031 569 0300	031 569 0420
Active Scanning CC	Mr A Brown	Postnet Suite 152 Private Bag X4 Bedfordview 2008	072 627 7259	011 616 5058
Structural Solutions CC	Mr R Govoni	PO Box 40295 Walmer 6065	041 581 3210	041 581 3126
UWP Consulting (Pty) Ltd	Dr A-C Brink	PO Box 13888 Cascades 3202	033 347 7900	033 347 7950
Bapedi Civil & Structural Consultants CC	Mr B Kunutu	PO Box 412689 Craighall 2024	011 326 3227	011 326 3363

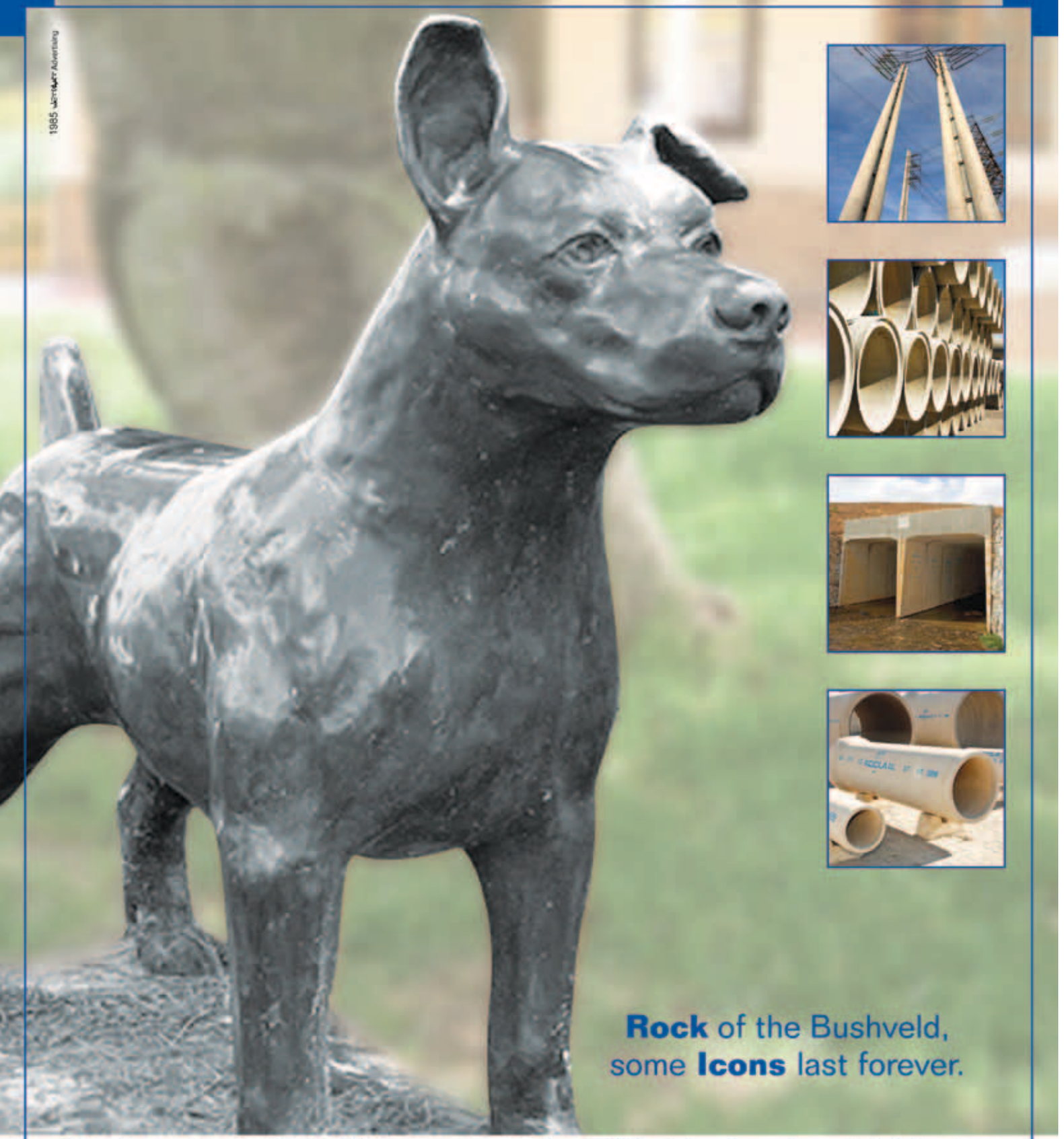

Rock of the Bushveld,
some **Icons** last forever.

Some legends really are built to last. Like our precast concrete products, ROCLA has the longevity, experience and technical expertise to see the job through. With over 91 years of unmatched experience, we could rightly call ourselves a South African Icon... ROCLA has an extensive network of factories throughout South Africa, Namibia and Botswana. We design and manufacture special products at customer requests.

ROCLA is ISO 9001/2008 certified and has the SABS mark of approval on all applicable products.

For technical expertise and unmatched experience, contact ROCLA now on Tel: (011) 670-7600 or Fax: (011) 472-2141. Web: www.rocla.co.za

ROCLA

OUR DIFFERENCE IS CONCRETE

Murray &Roberts

A Murray & Roberts Company

CONCRETE SOCIETY OF SOUTHERN AFRICA NATIONAL OFFICE PROGRAMME 2010			
DATE	**MEETING/EVENT**	**VENUE**	**CONVENOR**
End March	Concrete Beton Issue 124	Distributed to all members	Crown Publications
End April	2010/2011 Source Book	Distributed to all members	Crown Publications
End July	Concrete Beton Issue 125	Distributed to all members	Crown Publications
03 – 04 August	Concrete for a Sustainable Environment Symposium (CSE Symposium)	Emperor's Palace	CSE Symposium Organising Committee
05 August	Council Meeting	To Be Confirmed	CSSA President
10 October	Council Meeting	To Be Confirmed	CSSA President
Mid November	Concrete Flooring Roadshow Seminar	Durban, Port Elizabeth, Cape Town, Johannesburg	To Be Confirmed
End November	Concrete Beton Issue 125	Distributed to all members	Crown Publications

CONCRETE SOCIETY OF SOUTHERN AFRICA International Events Calendar 2010			
DATE	**MEETING/EVENT**	**VENUE**	**CONVENOR**
27 – 29 April	US- Africa Infrastructure Conference	JW Marriott Hotel, Washing DC, USA	Stephen Hayes
30 September – 01 October	6th "CCC" Central European Congress on Concrete Engineering	Marianske Lazne, Czech Republic	Vlastimil Sruma
26 – 28 November	Workshop on Optimisation of Construction Method for CFRD's	Pinghu Hotel, 53 Dongshan Road, Yichang, China	Chen Qian
17 – 22 January 2011	BAU 2011	New Munich Trade Fair Centre, Munich, Germany	Johannes Manger, Andrea Hack

CONCRETE SOCIETY OF SOUTHERN AFRICA WC BRANCH PROGRAMME 2010			
DATE	**MEETING/EVENT**	**VENUE**	**CONVENOR**
11 March	Western Cape AGM	UCT Chemical Engineering	Billy Boshoff
18 March	Annual Golf Day	Parow Golf Club	Riaan Brits
22 April	Site Visit	To be confirmed	Kevin Kimbrey
20 May	Monthly Technical Meeting	UCT Chemical Engineering	Etienne vd Klashorst
22 July	Site Visit	To be confirmed	Paul Zietsman
23 September	Cube Competition Casting Date	Else Fraser	
23 September	Site Visit	To be confirmed	Jerome Forturne
21 October	Cube Crushing Competition	University of Stellenbosch	Elsje Fraser
28 October	Monthly Technical Meeting	UCT Chemical Engineering	Hans Beushausen
18 November	Yearly Cocktail Party	CPUT Hotel School	Heinrich Stander